JMEPEG (2012) 21:2618–2621
DOI: 10.1007/s11665-012-0263-7

1059-9495/$19.00

Fracture of Polymer-Coated Nitinol During Gamma Sterilization

Dennis W. Norwich

(Submitted February 13, 2012; in revised form May 2, 2012)

After gamma sterilization of a packaged medical device, fractures were discovered in the superelastic nitinol wire used as part of the assembly. The nitinol wire was encased in fluorinated ethylene propylene (FEP) shrink tube. The only fractures occurred where the encased wire was held under strain during gamma sterilization. A study was conducted to determine the susceptibility of nitinol to this type of failure. The variables studied included wire diameter, wire surface finish, wire oxide layer, quantity of wires encased, type of tubing, and strain level during gamma sterilization. The greatest susceptibility to fracture occurred to single wire samples with a light oxide layer held under high strain in FEP shrink tube. Gamma sterilization experiments were conducted to isolate and confirm this failure mechanism. Scanning electron microscopy was used to analyze the fractured samples. Chemical analysis was performed in an attempt to detect trace elements to determine the root cause of the failures. Stress corrosion cracking caused by the liberation of fluorine due to the degradation of the polymer during gamma sterilization is suspected.

Keywords fluorine, fracture, gamma, halogen, nitinol, polymer, sterilization, stress corrosion cracking

1. Introduction

A medical device manufacturer reported fractures in the nitinol wires of a packaged and sterilized device during final device inspection. The nitinol component of this device consisted of 0.008″ diameter wires that were formed and heat treated in an air furnace. The wires were then encapsulated in fluorinated ethylene propylene (FEP) shrink tubing. The wires were then assembled to the rest of the device. To prepare the device for pouching, the wires were wrapped around the device handle. This wrapping caused a varying amount of strain in the nitinol wire. The pouched device was then sterilized by gamma irradiation to 30 to 50 kGy exposure. Poststerilization inspection revealed multiple fractures in the nitinol wire occurring only in the strained portion of the wire that was encapsulated in the FEP shrink tube. These results were verified and replicated in samples from multiple production lots, wire lots, and wire manufacturers. The following research reported in this paper is a result of an effort to determine the root cause of the noted wire fractures.

2. Material and Test Variables

An expanded study was designed to delve deeper into the phenomenon and determine the root cause of the fractures. The study focused on five variables: tubing polymer, strain level, wire diameter, quantity of wires encased in each tube, and wire surface finish (oxide level).

The following 13 polymers were tested: FEP, PTFE, PFA, ETFE, PVDF, PET, PEEK, PEBAX, polyolefin, polyurethane, polyethylene, polypropylene, and silicone.

Three strain levels were used: zero (straight wire), low (2% strain), and high (8% strain).

Two wire diameters were tested: ∅0.008″ (0.20 mm) and ∅0.021″ (0.53 mm).

Two quantities of wires encased in the tubing were used: one and four.

Three different wire surface finishes were tested. In order of increasing oxide layer thickness (measured by Auger analysis), they are: bright or oxide free (~100 Å oxide thickness), amber (~500 Å oxide thickness), and black (~2000 Å oxide thickness).

3. Sample Preparation

The samples for this research project were prepared to mimic the original occurence of failure. The wires were encased in the various tubings. The correct strain levels were achieved by winding the samples tightly around appropriately sized mandrels and securing the wire ends (see Fig. 1).

Strain was calculated using $\varepsilon = r/R \times 100\%$, where r is the radius of the wire and R is the radius of curvature to the neutral axis of the wire (Ref 1).

Groups of samples were bagged and labeled for gamma sterilization. Three runs of gamma sterilization were performed. The runs totaled 500 strained samples and 500 unstrained samples. The unstrained samples were used for fatigue testing to determine any latent effect of the sterilization on the fatigue life of the wire.

4. Postgamma Exposure Results

After 30 to 50 kGy of gamma irradiation over approximately an 18 h exposure duration, the samples were examined for

This article is an invited paper selected from presentations at the International Conference on Shape Memory and Superelastic Technologies 2011, held November 6-9, 2011, in Hong Kong, China, and has been expanded from the original presentation.

Dennis W. Norwich, Memry Corporation, Bethel, CT. Contact e-mail: dennis_norwich@memry.com.

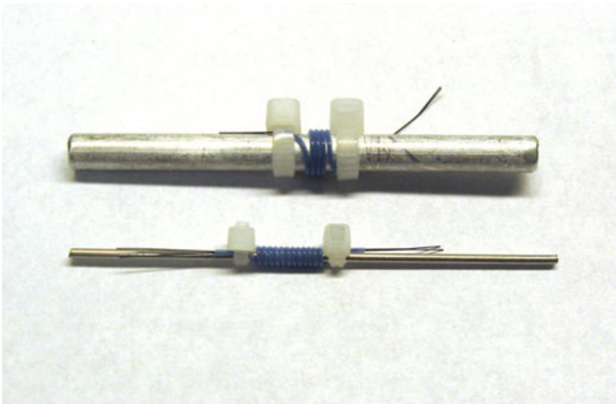

Fig. 1 Strained sample preparation

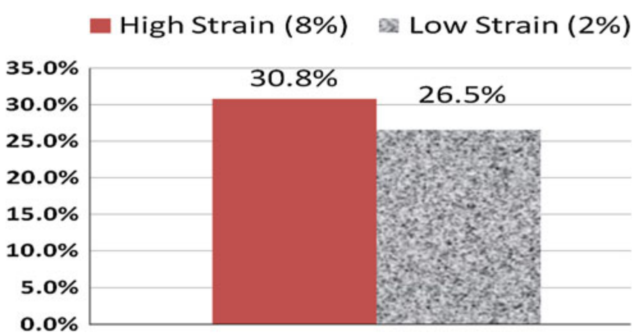

Fig. 2 Fractures by strain level, ∅0.008″ wire, single wire only, all oxide levels

fracture. The data were collated and graphed as shown in Fig. 2 to 6. For data collection purposes, a sample was counted as a fracture only once regardless of how many fractures occurred in the same sample. A summary of the results is listed below.

Polymer FEP was the only polymer in which fracture occurred. All the following data are for samples with FEP tubing only.
Strain High (8%) strain gave only a slightly higher fracture rate than the low (2%) strain (see Fig. 2).
Wire diameter The smaller (∅0.008″) wire diameter gave a much higher rate of fracture than the larger (∅0.021″) wire diameter (see Fig. 3).
Number of wires Single wire samples gave a much higher rate of fracture than multiple wire samples (see Fig. 4).
Wire surface finish Bright finish (the thinnest oxide layer) gave the highest rate of fracture (see Fig. 5).

Figure 6 depicts an FEP, high strain, ∅0.008″ wire, single wire, bright oxide sample. Note that the sample fractured into many pieces each approximately 3 mm in length. This combination of variables led to the highest rate of fracture for the nitinol wire.

5. Chemical and SEM Analysis

To determine if hydrogen embrittlement played a role in causing the fractures, samples were tested for hydrogen content by Vacuum Hot Extraction per ASTM E 146-83. The three groups tested were heat-treated wire, heat-treated wire with

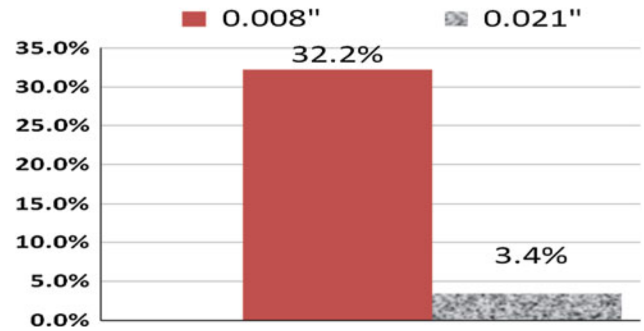

Fig. 3 Fractures by wire diameter, high and low strain, single wire only, all oxide levels

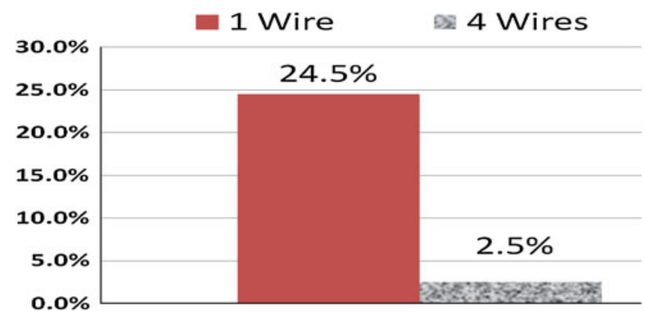

Fig. 4 Fractures by number of wires, high and low strain, ∅0.008″ wire, all oxide levels

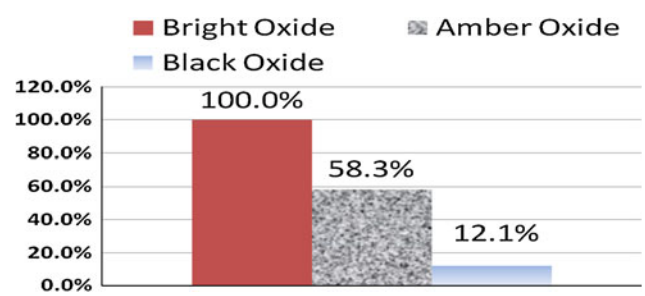

Fig. 5 Fractures by oxide level, high and low strain, single wire only, ∅0.008″ wire

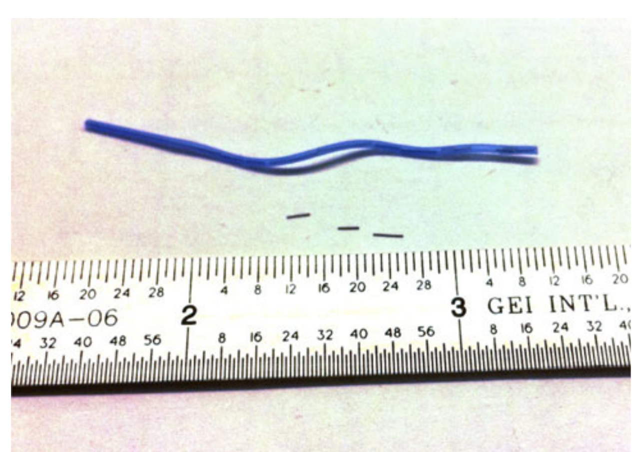

Fig. 6 Postgamma fracture

FEP shrink tube applied, and heat-treated wire with FEP shrink tube postgamma exposure and fracture. As we can see from the results in Table 1, the hydrogen content in all the three cases is too low to cause any level of embrittlement; therefore, another mechanism must be responsible for the fractures (Ref 2).

Scanning electron microscope (SEM) analysis was used to analyze the surface of samples that were fractured during gamma exposure (see Fig. 7). The image at first appears to be a fatigue-like fracture morphology (Ref 3). This is obviously not the case as the sample was fixed to the mandrel at all times.

This actually is a perfect example of stress corrosion cracking (SCC). SCC is a phenomenon most famously described by the British Army in the 1800s in India. The thin-walled necks of their cartridge cases cracked spontaneously during the monsoon season. The source of the problem was traced to a combination of high temperature and humidity, and traces of ammonia in the air (Ref 4).

The nitinol fractures reported here show a small discolored thumbnail initiation point with fatigue-like striations of propagation. The propagation is a result of a corrosive attack of the wire while under stress. The corrosion tunnel model proposes that the crack propagates through a series of steps of alternating tunnel growth and ductile fracture (Ref 5). The final fracture by overload is microvoid coalescence caused by stress concentration (Ref 3, 4).

6. Fatigue Testing

Fatigue testing was performed on the straight wire samples using a rotating beam fatigue tester (RBT). This is a zero mean strain test device. It can test up to 10 samples at a time with the wire guided in a test block machined with a radius to provide the desired strain level. Cycles to failure are recorded by a laser counter. The tests were performed in a 37 °C water bath at 1000 rpm. The water bath eliminates any heating effect created in the specimen due to dissipative processes during cyclic loading (cyclic stress induced formation of martensite). The heat transfer from the specimen to the test environment helps to counteract this process (Ref 6). The RBT test apparatus is shown in Fig. 8.

Fatigue life (ε-*N*) curves were generated for wire samples subjected to various combinations of FEP tubing, gamma irradiation, and strain. In Fig. 9, the three samples consist of a control wire that was not exposed to FEP tubing or gamma irradiation, a wire that was gamma irradiated without FEP tubing, and a wire that was encased in FEP tubing and aged for 4 months without gamma irradiation. We can see that the three curves lie on top of each other and all samples ran out at one million cycles at 0.6% strain; therefore, the FEP tubing or the gamma irradiation individually do not affect the fatigue life of the nitinol wire.

In Fig. 10, we again see the same control wire that was not exposed to FEP or gamma irradiation. It is plotted against wires with FEP that were gamma irradiated in a straight condition and wires with FEP that were gamma irradiated while being held at 0.5% strain.

Table 1 Hydrogen content analysis

Condition	Hydrogen content, ppm
Heat-treated wire	11
PostFEP shrink tube	12
Postgamma fracture	20

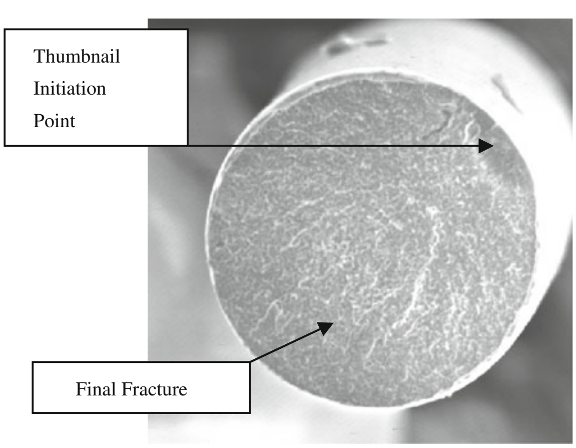

Fig. 7 SEM Image of postgamma SCC

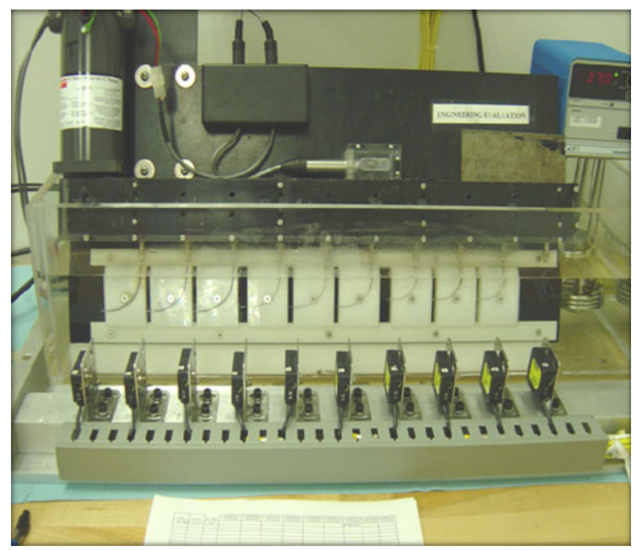

Fig. 8 Rotating beam test apparatus

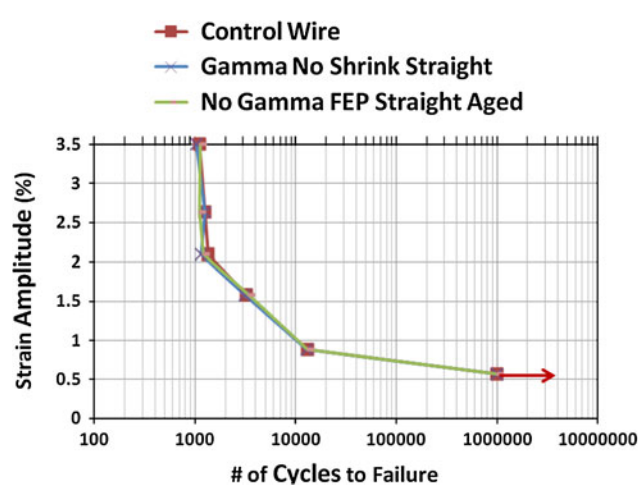

Fig. 9 Strain-N NiTi control samples

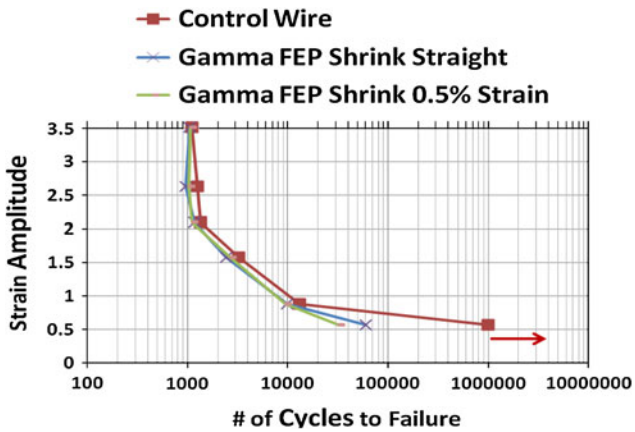

Fig. 10 Strain-N NiTi irradiated with FEP

The results show the latency of the exposure to irradiated FEP. Even without fracture, there is a drastic reduction of fatigue life caused by the irradiated FEP. The average fatigue failure at 0.6% strain dropped from run out at one million cycles to failure at 60,000 cycles. This is exacerbated by holding the wires under 0.5% strain during irradiation where the fatigue failure at 0.6% strain dropped to 32,000 cycles.

7. Discussion and Conclusions

The demonstrated data lead to the following observations:

- NiTi is subject to fracture when encased in FEP and strained during gamma sterilization.
- If the wire does not fracture or is not strained there is still a latent reduction in fatigue life of the wire.
- A thinner oxide layer on the wire greatly magnifies the fracture effect.
- Smaller wire diameters or fewer wires magnify the fracture effect.

These observations agree with the facts that FEP is known to degrade during gamma sterilization and nitinol is known to be susceptible to damage by halogens (Ref 7, 8). The degradation of the FEP leads to a fluorine (F−) or hydrofluoric acid (HF) by-product that attacks the nitinol propagating the failure by alternating corrosion tunnel growth and ductile fracture causing SCC (Ref 4). Most of the F− or HF would dissipate and be difficult to detect in later laboratory analysis. The limited gamma-induced harmful by-products spread their attack on the nitinol over the entire surface area of the Nitinol encased in the FEP tubing. This explains why single wires and smaller diameter wires are most affected. A larger wire surface area will spread out the effect and reduce fracture potential.

Strain and a thinner oxide layer allow easier penetration of the harmful by-product. SCC is known to form at slip steps so the strain-induced martensitic transformation accelerates the phenomenon (Ref 4).

Concurrent research by M. Drexel, S. Smith et al. presented at SMST 2011 has shown SCC in nitinol encased in FEP and PTFE tubing after electron beam sterilization (Ref 9).

Any application containing nitinol along with a halogenated polymer should be thoroughly reviewed and tested before specifying any irradiated sterilization method.

References

1. D. Norwich and A. Fasching, A Study on the Effect of Diameter on the Fatigue Properties of NiTi Wire, *SMST-2008 Proceedings of the International Conference on Shape Memory and Superelastic Technologies*, A. Tuissi, M. Mitchel, and J. San Juanm stress corrosion cracking, Ed., Stresa, Italy, 2009, p 558–562
2. A. Thompson and N. Moody, Ed., *Hydrogen Effects in Materials*, TMA, Warrendale, PA, 1996, p 699–840
3. B. James, S. Murray, and S. Saint, Fracture Characterization in Nitinol, *SMST-2003 Proceedings of the International Conference on Shape Memory and Superelastic Technologies*, A. Pelton and T. Deurig, Ed., Pacific Grove, CA, 2004, p 321–324
4. H. Chandler, *Metallurgy for the Non-Metallurgist*, ASM International, Materials Park, OH, 1998, p 185–196
5. S. Cramer and B. Covino, Ed., *Corrosion: Fundamentals, Testing, and Protection, ASM Handbook*, Vol. 13A, ASM International, Materials Park, OH, 2003, p 346–366
6. M. Wagner, T. Sawaguchi, G. Kaustrater, D. Hoffken, and G. Eggeler, Structural Fatigue of Pseudoelastic NiTi Shape Memory Wires, *Materials Science and Engineering*, 2004, **A378**, p 105–109
7. L. Massey, *The Effects of Sterilization Methods on Plastics and Elastomers*, William Andrew Publishing, Norwich, NY, 2005, p 1–60
8. P. Adler, S. Herreria, G. Kostur, S. Carpenter, P. Poncet, M. Wu, and W. DiScipio, The Role of Alkaline Cleaning Solutions and Cl- Containing Lubricants on Pitting Corrosion in NiTi Alloys, *SMST-2003 Proceedings of the International Conference on Shape Memory and Superelastic Technologies*, A. Pelton and T. Deurig, Ed., Pacific Grove, CA, 2004, p 385–392
9. M. Drexel, S. Smith, B. Gause, and D. Plumley, Irradiation-Assisted Stress-Corrosion Cracking of Nitinol During eBeam Sterilization, *The International Conference on Shape Memory and Superelastic Technologies*, Hong Kong, China, 2011